Bioorganic Chemistry 89 (2019) 103023

Contents lists available at ScienceDirect

Bioorganic Chemistry

journal homepage: www.elsevier.com/locate/bioorg

Design, synthesis, modeling studies and biological screening of novel pyrazole derivatives as potential analgesic and anti-inflammatory agents

Azza T. Taher[a,b], Marwa T. Mostafa Sarg[c], Nermeen R. El-Sayed Ali[d], Noha Hilmy Elnagdi[e,*]

[a] Cairo University, Faculty of Pharmacy, Pharmaceutical Organic Chemistry Department, Cairo, Egypt
[b] October 6 University (O6U), Faculty of Pharmacy, Pharmaceutical Organic Chemistry Department, 6th of October City, Giza, Egypt
[c] Al-Azhar University, Faculty of Pharmacy, Organic Chemistry Department (Girls), Cairo, Egypt
[d] Misr University for Science and Technology, Faculty of Pharmacy, Organic Chemistry Department, Giza, Egypt
[e] Modern University for Technology and Information, Faculty of Pharmacy, Organic Chemistry Department, Cairo, Egypt

ARTICLE INFO

Keywords:
Pyrazole Floctafenine
Anti-inflammatory
Analgesic
Chalcones
Indomethacin
Docking
Molecular modeling study

ABSTRACT

Reported herein are the design, synthesis, and pharmacologic evaluation of novel pyrazole and pyrazoline derivatives. The study presents the effect of lengthening of carbon chain in different pyrazole derivatives bearing various amine moieties. Combination of pyrazoline ring with either pyrazole or quinoline rings (Floctafenine derivatives) through synthesis of chalcones and their cyclization into pyrazolines was involved. The structures of target compounds were confirmed by elemental analysis and spectral data. All the newly synthesized compounds were investigated for their anti-inflammatory and analgesic activities compared to Indomethacin as a reference drug. Docking and molecular modeling study was initiated to validate the attained pharmacological data and provide understandable evidence for the observed anti-inflammatory behavior of the most potent compounds **14b**, **15b** and **22** through their various interactions with the active site of COX-2 isozyme. Protein Data Bank (PDB) file of COX II enzyme with the code **4Z0L** and its co-crystallized ligand Indomethacin were used for this purpose. The binding affinity was evaluated via comparing the scoring energy (S) and amino acid interactions of novel compounds with Indomethacin.

1. Introduction

Inflammation is a complex biological process and many enzymes are involved such as NO synthetase and COX-2. Inflammation can be triggered by a variety of factors, including pathogens, damaged cells and toxic compounds. Abnormal activation of certain enzymes, such as superoxide dismutase (SOD), glutathione peroxidase (GPx), high-mobility group box 1 (HMGB1), NADPH oxidase (NOX), inducible nitric oxide synthase (iNOS) and cyclooxygenase (COX)-2, are of the main reasons for the development of inflammation-related diseases, such as cardiovascular disease and cancer [1,2]. Non-steroidal anti-inflammatory drugs (NSAIDs) are considered to be the most commonly used therapeutics for the treatment of pain and inflammation through inhibition of the biotransformation of arachidonic acid to prostaglandins (PGs), prostacyclin (PGI2), and thromboxane A2 (TXA2) via cyclooxygenase (COX) enzymes (COX-1, -2) [3–6]. However, NSAIDs have many adverse effects, including gastrointestinal bleeding [7], cardiovascular side effects [8–10], increased the risk of atherothrombosis [11], and NSAID induced nephrotoxicity [12–15]. Some cardiovascular side effects such as myocardial infarction led to the withdrawal of rofecoxib and valdecoxib from the market [16]. This has urged scientists to continuously develop analogues for NSAIDs in trials to improve the drugs' biological activity and diminishing side effects [17].

Pyrazole nucleus possesses almost all types of pharmacological activities as anti-inflammatory and analgesic activities in addition to antimicrobial, antidiabetic, antiviral, anticancer, anti-hypertensive and MAO-B inhibitory activities [18–30]. Pyrazolo[4,3-*c*]quinolines derivatives were reported recently as potential anti-Inflammatory agents through inhibition of inducible nitric oxide synthase (iNOS) and cyclooxygenase 2 (COX-2) protein expression [31]. Some examples of pyrazole derivatives such as SC-558, Deracoxib, Famprofazone, Ramifenazone, Fipronil, Rimonabant and Pyraclonil have been reported as potent NSAIDs [32] Fig. 1.

Accordingly, our efforts were devoted to synthesize and biologically evaluate a number of novel pyrazole derivatives having potent anti-inflammatory and analgesic activities as analogues to the well known drugs, Celecoxib (Celebrex®) and Lonazolac (Irritern®) [33,34]with the

* Corresponding author at: Organic Chemistry Department, Faculty of Pharmacy, Modern University for Technology and Information, Cairo, Egypt.
E-mail address: Elnagdinoha@yahoo.com (N. Hilmy Elnagdi).

https://doi.org/10.1016/j.bioorg.2019.103023
Received 8 April 2019; Received in revised form 19 May 2019; Accepted 29 May 2019
Available online 31 May 2019
0045-2068/

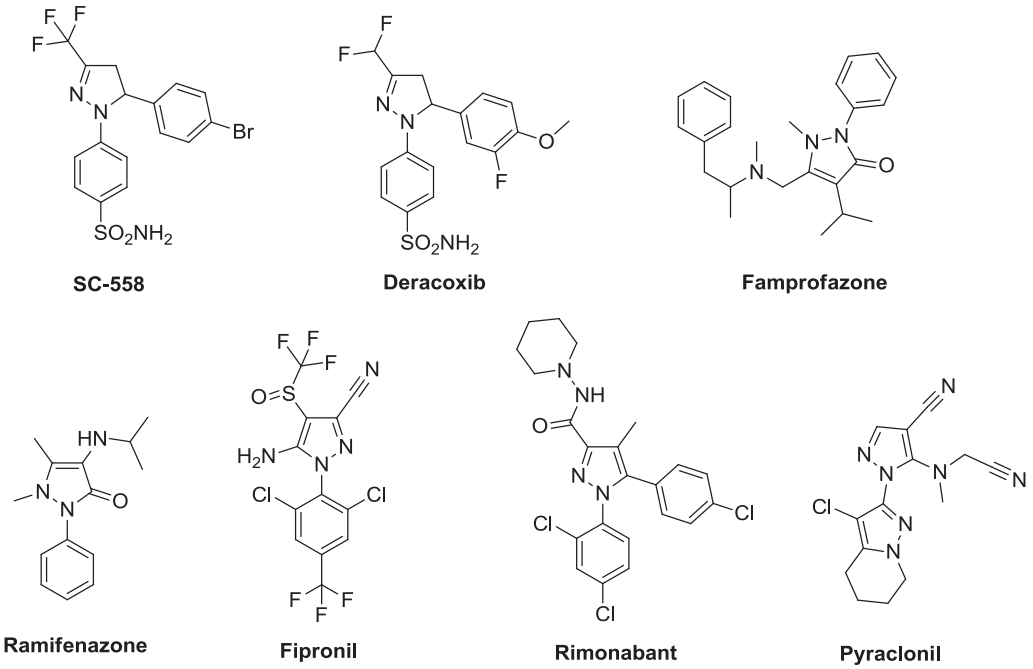

Fig. 1. Examples of pyrazole derivatives reported as potent NSAIDs.

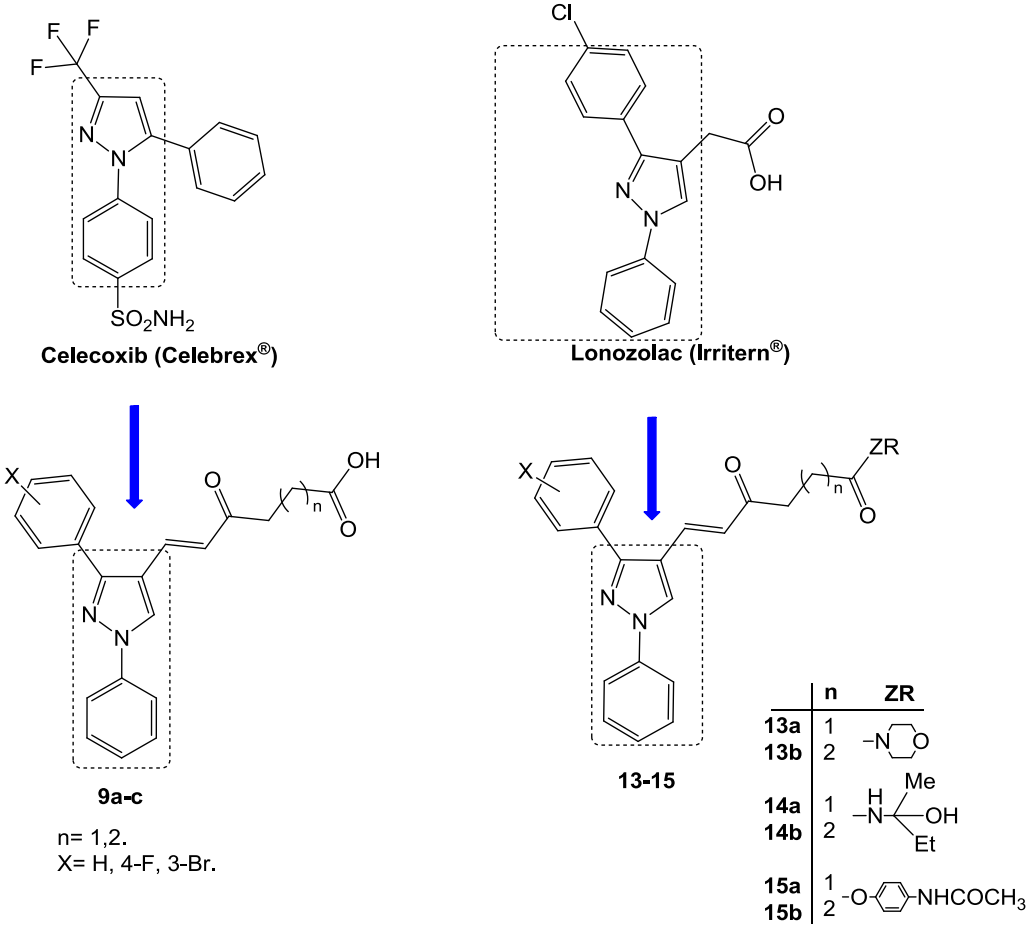

Fig. 2. Similarities between Celecoxib (Celebrex®) and Lonazolac (Irritern®) and our synthesized target molecules 9, 13, 14, 15.

hope of improving biological activity and diminishing side effects Fig. 2. Accordingly, the anti-inflammatory and analgesic activities of the newly synthesized compounds were estimated. It has been reported that Indomethacin (Indomethacin®) had been converted to selective analogue simply through the transformation of the carboxylic acid moiety to amide functional to produce Indomethacin amide [35,36] Fig. 3. Therefore; reduction of the acid chain of compounds **9a,b** was achieved by converting it into amides **13a,b** and **14a,b** using

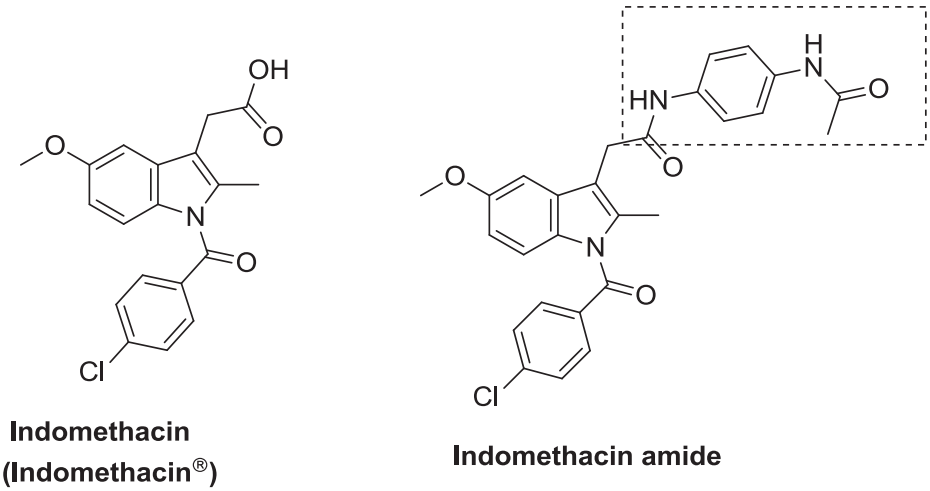

Fig. 3. Indomethacin and Indomethacin amide as potent NSIADs.

morpholine and 2-amino-2-methylpropanol, respectively with the hope to go a step further in the field of COX-2 selective anti-inflammatory and analgesic agents. On the other hand, it was planned to design compounds bearing ester linkage **15a,b** instead of amidic one present in Indomethacin amide. This was achieved by using *N*-(4-hydroxyphenyl) acetamide (paracetamol marketed as paramol®) which is already existing in the market as a potent analgesic drug [37].

It has been reviewed that pyrazoline derivatives as Ramifenazone **D** showed potent non steroidal anti-inflammatory activity [38]. In addition,literature survey revealed that combination between pyrazole and pyrazoline nuclei enhance both anti-inflammatory and analgesic activities [39]. Therefore, pyrazoles bearing pyrazoline ring were designed in order to obtain better pharmacological activities. Furthermore, our interest was extended to investigate the anti-inflammatory/analgesic activities of chalcone derivative **21** of Floctafenine marketed as Idrac® bearing quinoline nucleus which has been reported to exhibit both activities [40] (Fig. 4). Floctafenine pyrazoline **22** also were prepared by cyclization of chalcones which exhibits potent anti-inflammatory/analgesic activities.

The integrity of the structures of the newly synthesized compounds would be substantiated by microanalyses, IR, ^{1}H NMR, and MS data. Furthermore, molecular modeling concept was adopted in an attempt to gain a better insight on the molecular interactions and to help in understanding the mode of action of the active compounds through their interactions with the active sites of COX-2 isozymes.

2. Results and discussion

2.1. Chemistry

The first synthesis of substituted pyrazoles was carried out in 1883 by Knorr *et al.* who reacted 1,2-diketones with hydrazines to give two regioisomers [41]. Since then many synthetic routes were reported for the synthesis of pyrazole and its derivatives attempting more regioselectivity for the products thus increasing the yield of the targeted molecules [30]. Among the most successful is the Vilsmeier–Haack synthesis of pyrazoles via the reaction of phenyl hydrazines with aldehydes or ketones [42–48]. Thus in this work pyrazoles **7a-c** were prepared via the reaction of phenyl hydrazine **1** with aromatic ketones **2a-c** in refluxing ethanol/CH_3COOH mixture followed by the addition of two equivalents of dimethyl formamide and $POCl_3$. Although the mechanism of the Vilsmeier–Haack reaction is not certain; we suggest that the reaction mechanism proceeded as shown in Scheme 1, where initially phenyl hydrazone **1** reacted with ketones **2a-c** to afford phenyl hydrazones **3a-c**. This is followed by the reaction of **3a-c** with two equivalents of dimethyl formamide and phosphorous oxychloride mixture at the active methylene group of the hydrazone **1,** followed by cyclization with loss of dimethyl amine group, then hydrolysis with loss of another and formylation to afford **7a-c**. This method proved to be greener than that reported from 1,3-diketones as it is regioselective, time saving, and of high yield (90–95% yield).

In present work, also target molecules **9a-f** were prepared in good yields through δ-condensation of the appropriate pyrazole aldehyde **7a-c** with either levulinic acid **8a** to yield compounds **9a-c** or by the

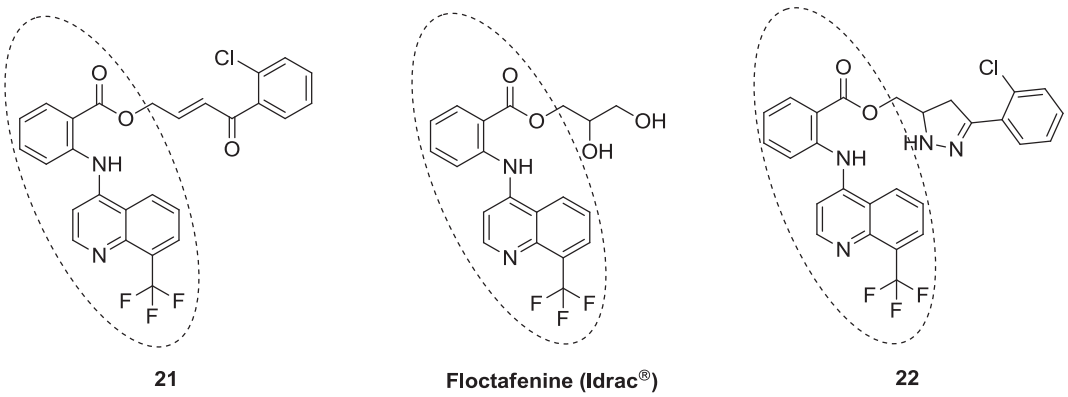

Fig. 4. Feature similarities between Floctafenine (Idrac®) and target compounds **21** and **22.**

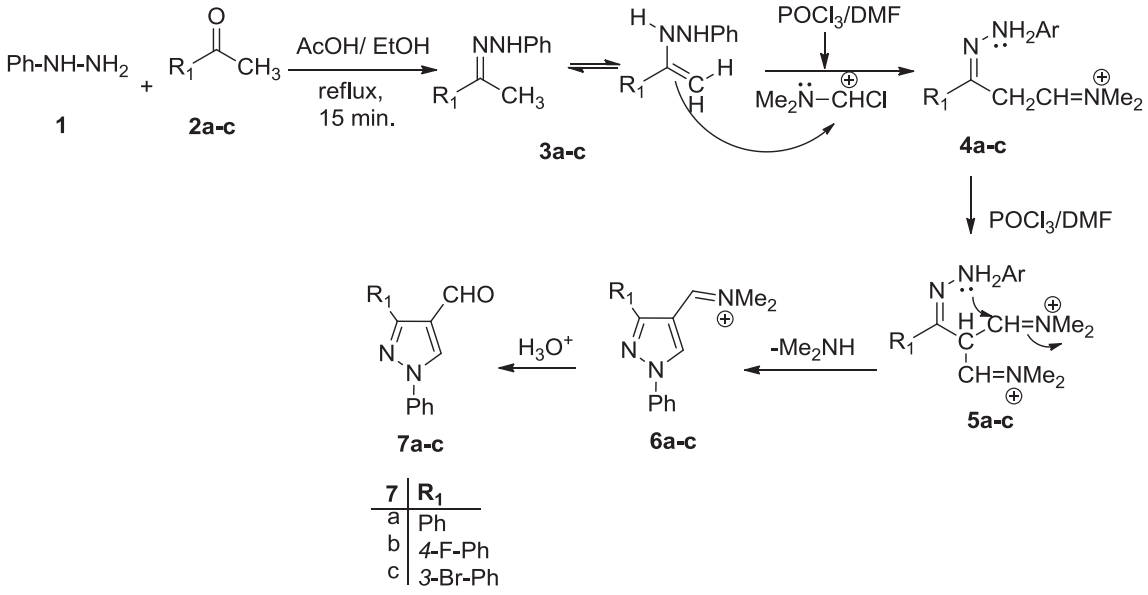

Scheme 1. Preparation of pyrazole aldehydes **7a-c.**

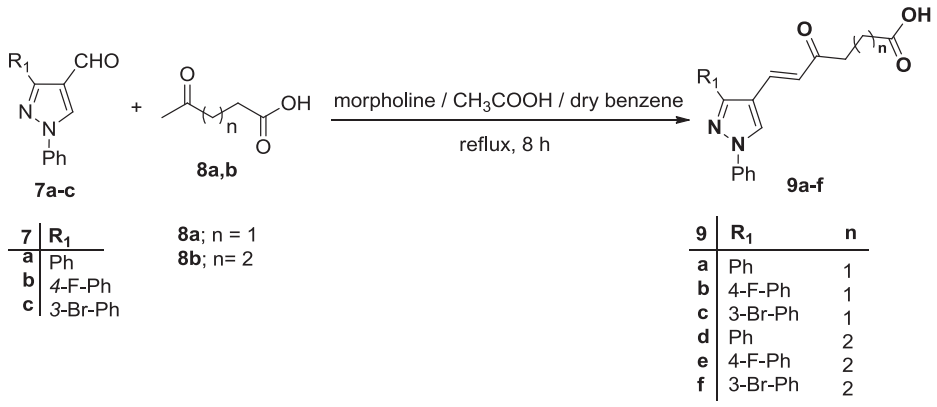

Scheme 2. Preparation of the pyrazole carboxylic acids **9a-f.**

reaction of **7a-c** with 4-acetylbutyric acid **8b** to afford compounds **9d-f** in presence of either of 5% alcoholic sodium hydroxide or a mixture of glacial acetic acid in piperidine or morpholine 30 in the ratio 3:1 in Dean Stark apparatus [49–51] (Scheme 2).

The supporting evidences of compounds **9a-f** were confirmed by microanalyses and spectral data. The ^{1}H NMR spectra of compounds **9b** and **9c** indicated the presence of two triplets at δ 2.10–2.74 ppm and δ 2.74–2.97 ppm each integrated for two protons attributed to levulinic acid $-CH_2$ protons. In addition to two doublets at δ 6.50–6.66 ppm and δ 6.79–7.20 ppm each integrated for one proton corresponding to two arylidene protons and a deuterium oxide exchangeable singlet at δ 7.61–8.15 ppm due to carboxylic OH protons. The **^{1}H NMR** spectra of compounds **9d** showed three triplets at δ 1.99 ppm, δ 2.46 ppm and δ 2.71 ppm each integrated for two protons corresponding to butyric acid $-CH_2$ protons, besides, two doublets at δ 6.57 ppm and δ 6.63 ppm attributed to the two arylidene protons and a deuterium oxide exchangeable singlet at δ 7.33 ppm due to carboxylic OH function.

Our target molecules were prepared via reaction of the pyrazole acid derivatives **9a or 9d** with either morpholine **10**, 2-amino-2-methyl-1-propanol **11** or paracetamol **12** in dry CH_3Cl, ethyl chloroformate, triethyl amine and stirring at room temperature for 24 h to produce the corresponding amides **13a,b, 14a,b** and esters **15a,b** respectively [51] (Scheme 3).

Then we shifted to synthesis of chalcone analogues as our target molecules. Generally chalcones are prepared via Claisen-Schmidt condensation under conventional heating [52–55] or microwave assisted reaction [56]. Initially the reaction of **7a,b** and 2-chloro acetophenone in absolute ethanol containing potassium hydroxide as a base afforded the chalcone analogues **17a,b** in good yields. This was followed by refluxing chalcone derivatives **17a,b** and 99% hydrazine hydrate in absolute ethanol to afford the bipyrazoles**18a,b** (scheme 4).

Supporting evidence of the structure **17a,b** was confirmed by; **IR** spectra which showed that absorption bands ranged from 1666 cm^{-1} corresponding to carbonyl group. The **^{1}H NMR** spectrum pointed to the appearance of olefinic protons at δ 7.25 ppm. Other protons appeared at their expected chemical shifts.

The **IR** spectra of **18a** and **18b** lacked the absorption bands of carbonyl functions of the precursor and displayed absorption bands at 3439–3427 cm^{-1} corresponding to NH functions. Other bands appeared at expected frequencies. The **^{1}H NMR** spectra of compound **18b** revealed multiplet at δ 1.13–1.20 ppm corresponding to pyrazoline CH_2 protons and multiplet at δ 3.91–3.97 ppm corresponding to pyrazoline C_5-H; respectively. In addition to an exchangeable singlet at δ 6.75 ppm disclosing the presence of NH function. The electron impact mass spectrum of compound **18b** revealed the molecular ion peak at *m/z* 416.00 (M^+, 8.20) and the base peak at *m/z* 78.00 (100).

The intermediate 2-oxoethyl 2-[(8-(trifluoro methyl)quinolin-4-yl) amino]benzoate **20** was synthesized from 2,3-dihydroxypropyl-2-(8-(trifluoromethyl)quinolin-4-ylamino)benzoate which is commercially

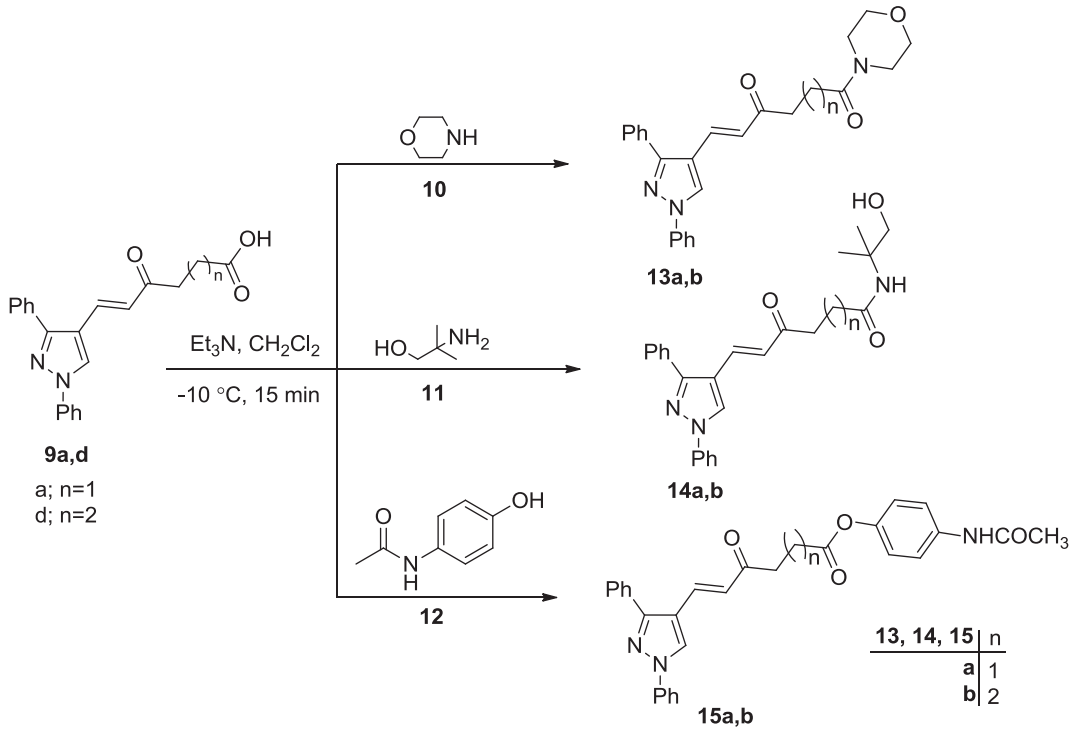

Scheme 3. Preparation of pyrazole amides **13a,b**, **14a,b** and pyrazole esters **15a,b.**

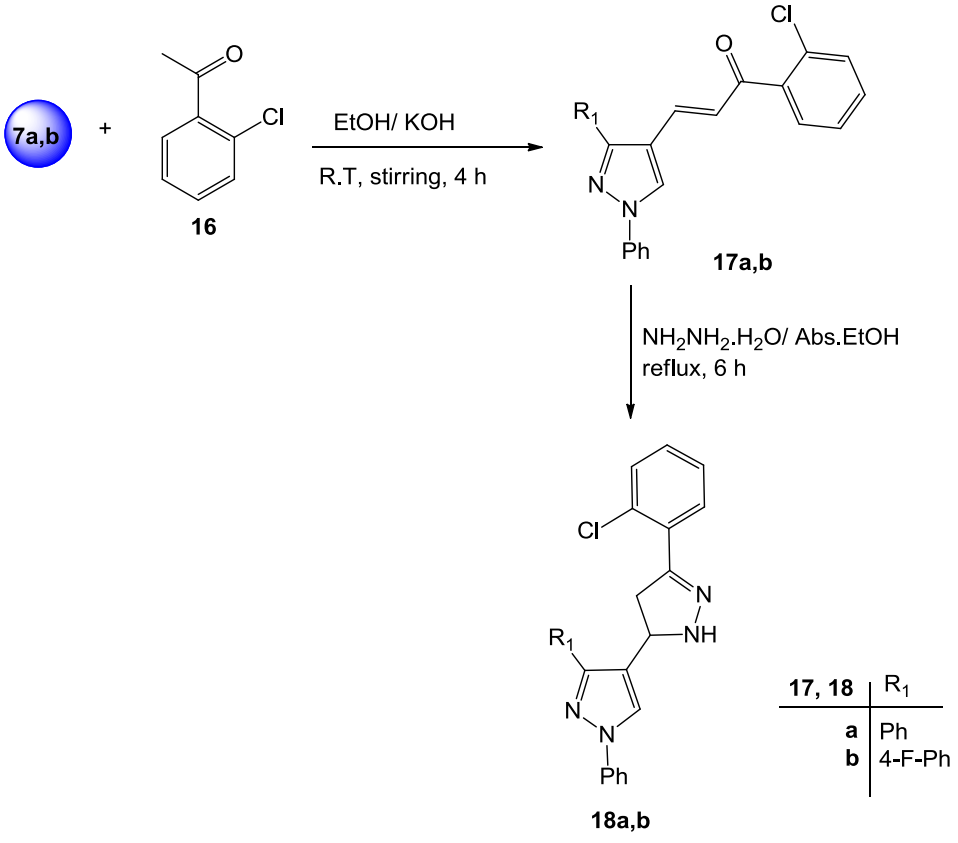

Scheme 4. Preparation of the pyrazole chalcones **17a,b** and bipyrazoles**18a,b.**

available as Idrac® **19** by stirring the latter with potassium periodate in presence of glacial acetic acid at room temperature for 15 min [20,40]. In the present work, the desired chalcone 4-oxo-4-(2-chlorophenyl)but-2-enyl 2-(8(trifluoromethyl)quinolin-4-ylamino)benzoate **21** was synthesized via Claisen-Schmidt condensation of compound **20** with the 2-chloroacetophenone in potassium hydroxide (scheme 5).

The **^{1}H NMR** spectra of compound **21** revealed the presence of olefinic protons of chalcone moiety which appeared at

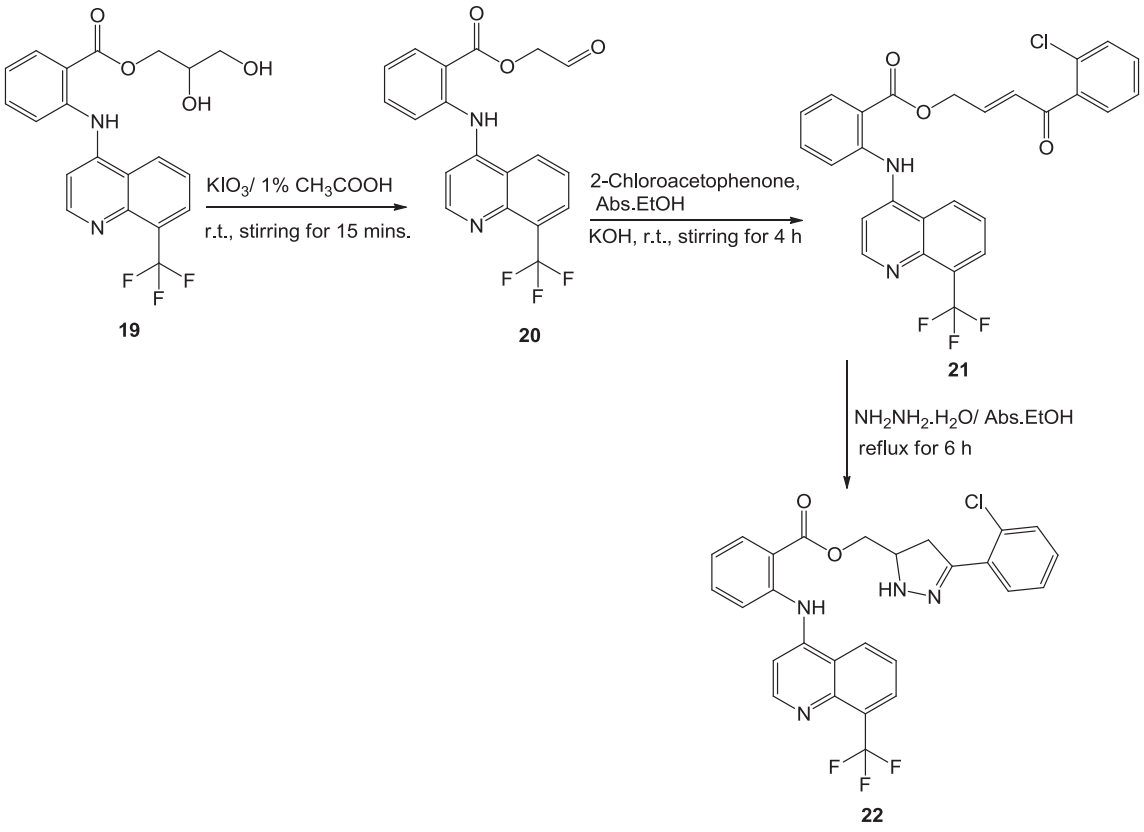

Scheme 5. Preparation of Floctafenine chalcone **21** and pyrazoline **22.**

δ = 6.34–7.16 ppm. Other protons appeared at their expected chemical shifts. The electron impact mass spectrum revealed peaks at *m/z* 512.00 (M + 2, 1.86) and *m/z* 78.00 (100). Finally, the target compound methyl (4,5-dihydro-3-(2-chlorophenyl)-1*H*-pyrazole-5-yl)-2-(8-(trifluoromethyl)quinolin-4-ylamino)benzoate **22** was synthesized via the reaction of the chalcone **21** with 99% hydrazine hydrate in absolute ethanol under reflux conditions. The **^{1}H NMR** spectra of compound **22** showed three multiplets at δ 1.23–1.28 ppm pointed to pyrazoline–CH_2 protons. In addition to other multiplets at δ 3.72–3.75 ppm integrated for three protons attributed to pyrazoline-C_5 and OCH_2 protons. Besides to, deuterium oxide exchangeable singlets at δ 6.42–6.92 ppm corresponding to pyrazoline-NH proton, in addition to other exchangeable singlets at δ 9.05–9.90 ppm pointed to quinoline-NH proton.

2.2. Anti-inflammatory effect

It was observed that compounds **14b**, **15b** and **22** possessed significant anti-inflammatory activity (28.57–30.95%) in which the **14b** give the same potency of reference drug **Indomethacin** (Indomethacin®) (30.95%). The spacer (aliphatic chain composed of either two methylene groups in levulinic derivatives or three methylene groups in butyric analogues) had a marked role in anti-inflammatory activity.

As revealed from the results presented in (Table 1**)**; lengthening of aliphatic chain in **13b**, **14b** and **15b** (26.19%, 30.95% and 28.57%); respectively led to higher activity when compared to their levulinic analogues **13a**, **14a** and **15a** (23.81%, 19.05%, 26.19%); respectively. Compounds **13**, **14** and **15** possessed significant anti-inflammatory activity, this may be attributed to great reduction in acidic character by converting the free carboxylic acid group to amide or ester functions through their reaction with amines such as morpholine [35] , 2-amino-2-methyl-1-propanol [63], or *N*-(4-hydroxyphenyl)acetamide [57] which were reported to have anti-inflammatory and analgesic activities. Moreover, combination between pyrazoline ring and highly effective quinoline ring of Floctafenine [58] gave compound with significant results **22**. In addition, cyclization of chalcones **17** and **21 (**9.52% and 4.76%; respectively) into pyrazolines **18a** and **22** (21.43%, 28.57%; respectively) led to marked increase in oedema inhibition (see Table 1 and Fig. 5)

2.3. Analgesic activity studies

It was observed that the percentage inhibition of writhing movements of the synthesized compounds ranged from **89.7 to 39.7%** in comparable to the reference drug Indomethacin (Indomethacin®) **94.8%**. Additionally, length of aliphatic chain in propanol amides **14a** and **14b** did not show difference in the analgesic activity **51.7%**, however, it increased the activity in levulinic morpholine amide **13a** in comparable to its butyric analogue **13b** (**56.9%** and **39.7%**; respectively). Paracetamol ester with longer carbon chain **15b** gave higher analgesic activity **50%** than its levulinic analogue **15a 46.6%.** Moreover, the combination of pyrazoline nucleus with quinoline ring in Floctafenine derivatives **21** and **22** exhibited the highest analgesic activity among all the tested compounds (**75.9%** and **84.5%**; respectively) (Table 2).

2.4. Docking studies

Based on the results of the anti-inflammatory activity, docking of the most active compounds (**14b, 15b** and **22**) and the positive control **Indomethacin**, was performed with binding site of COX-2 (PDB ID: 4Z0L**)** to shed light on their potential binding modes and investigate their similarity to the standard ligand binding modes [59].

Table 3 and Figs. 6–13 illustrate the results and the bonding interactions of the docked compounds **14b, 15b, 22** and **Indomethacin** the positive control respectively, with amino acids of the active site.

Table 1
Anti-inflammatory evaluation of tested compounds (Paw oedema test).

Comp. no.	At zero time Mean ± S.D.	% oedema inhibition	1 Hour Mean ± S.D.	% oedema inhibition	2 Hours Mean ± S.D.	% oedema inhibition	4 Hours Mean ± S.D.	% oedema inhibition
13a	3.60 ± 0.89	10.00	3.80 ± 0.76	24	3.55 ± 0.27	21.11	3.20 ± 0.27	23.81
14a	3.40 ± 0.55	15.00	4.40 ± 0.89	12	3.60 ± 0.55	20	3.40 ± 0.55	19.05
15a	3.60 ± 0.55	10.00	4.10 ± 0.89	10	3.70 ± 0.45	17.78	3.10 ± 0.22	26.19
13b	3.40 ± 0.55	15.00	4.00 ± 0.35	20	4.10 ± 0.42	8.89	3.10 ± 0.22	26.19
14b	3.90 ± 1.14	2.50	3.00 ± 0.35	40	3.35 ± 0.42	25.56	2.90 ± 0.22	30.95
15b	3.40 ± 0.89	15.00	4.00 ± 0.50	20	3.80 ± 0.45	15.56	3.00 ± 0.61	28.57
17a	3.60 ± 0.55	5.26	4.80 ± 0.84	4	3.80 ± 0.84	15.56	3.80 ± 0.84	9.52
18a	3.10 ± 0.55	22.50	3.60 ± 0.42	28	4.00 ± 0.50	11.11	3.10 ± 0.22	26.19
18b	3.00 ± 0.01	25.00	3.50 ± 0.50	30	4.30 ± 0.45	4.44	3.30 ± 0.27	21.43
21	4.20 ± 0.84	–	4.6 ± 0.89	8	4.00 ± 1.00	11.11	4.00 ± 0.71	4.76
22	3.60 ± 0.42	10.00	3.20 ± 0.45	36	3.80 ± 0.84	15.56	3.00 ± 0.71	28.57
Control	4.00 ± 0.45	–	5.00 ± 0.71	–	4.50 ± 0.71	–	4.20 ± 0.84	–
Indomethacin	2.90 ± 0.65	23.68	3.00 ± 0.71	40	3.20 ± 0.45	28.89	2.90 ± 0.42	30.95

The data represents the mean ± standard error of the mean (n = 5). Values represent the mean ± S.E. of five animals.

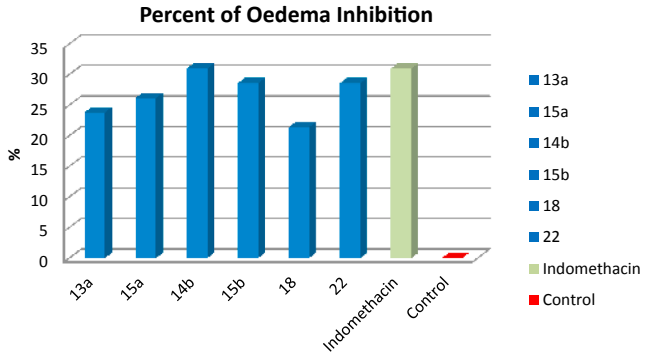

Fig. 5. Percent of oedema inhibition after four hrs for the most active compounds.

Table 2
Analgesic evaluation of tested compounds (Writhing test).

Comp. no.	Mean of no. of writhing movements	% Inhibition (analgesic activity)
13a	5.0	56.9
14a	7.0	39.7
15a	5.6	51.7
13b	5.6	51.7
14b	6.2	46.6
15b	5.8	50.0
17	3	74
18	2.8	75.9
21	1.2	89.66
22	1.8	84.5
Control	11.6	–
Indomethacin	0.6	94.8

Generally, the tested compounds and **Indomethacin** showed comparable binding pattern and equal docking score can be used to compare the binding affinity of different ligands to the same protein. Docking of Indomethacin into COX-2 active site revealed that several interactions were considered to be responsible for the observed affinity of the compound as S = −14.141 Kcal/mol as it acts as a hydrogen bond acceptor through two hydrogen bonds via both the oxygen atoms of carbonyl group and Arg 120 (3.17 Å and 2.91 Å) as shown in Figs. 6 and 7. Compound **14b** exhibited the highest binding affinity to the active site pocket with S = −16.390 Kcal/mol among the tested compounds as it interacted as hydrogen bond acceptor via carbonyl group with Arg 120 (2.72 Å and 3.02 Å) and as pi-H via diazole ring with two amino acid residues Val349 (3.71 Å) and Ala527 (4.15 Å) as shown in Figs. 8 and 9. Docking energy (S = −16.270 Kcal/mol) of compound **15b** showed a unique binding to Arg513 and that it exerted high binding affinity, which can be explained by several interactions with three amino acid residues. It acted as hydrogen bond acceptor via oxygen atoms of carbonyl group with Arg120 (2.83 Å) and with Arg 513 through two hydrogen bonds (2.82 Å and 2.70 Å). Additionally, it interacted as a H-donor with Ser118 (2.74 Å) via NH group and with Ala527 (4.11 Å) via diazole ring as cleared in Figs. 10 and 11. Compound **22** interacted with COX-2 active site with S = −13.400 Kcal/mol as it acted as a hydrogen bond acceptor via oxygen atom of carbonyl group with Arg120 (2.99 Å) as shown in Figs. 12 and 13.

3. Conclusion

Our novel pyrazole and pyrazoline derivatives showed marked anti-inflammatory activity and analgesic activities. The results suggested that the length of carbon chain plays an important role in both anti-inflammatory and analgesic activities. The lengthening of carbon chain in compounds **13b**, **14b** and **15b** gave higher anti-inflammatory activities comparable to their levulinc acid derivatives. Combining the pyrazole with amide or ester functions through their reaction with amines as morpholine, 2-amino-2-methyl-1-propanol, or *N*-(4-hydroxyphenyl)acetamide led to potent anti-inflammatory and analgesic pyrazole derivatives. Cyclization of chalcones into pyrazolines gave more potent anti-inflammatory in compounds **18** and **22** and higher analgesic activity in compound **18**. Additionally, combination between pyrazoline ring and quinoline ring in Floctafenine derivative afforded compound **22** with marked activity as both anti-inflammatory and analgesic agent. Finally, compound **14b** had the highest binding affinity among the selected compounds which was compatible with the results of anti-inflammatory evaluation study. The docking results illustrated that the interaction with the active site involved five amino acid residues (**Arg120**, **Arg513**, **Ser119**, **Val349, and Ala527**) with accepted lengths of hydrogen bonds which were reported to be responsible for potent anti-inflammatory activity.

4. Experimental section

4.1. Chemistry

Melting points were determined in Stuart apparatus and the values given are uncorrected. IR spectra were recorded, for potassium bromide discs, on a Shimadzu IR 435 spectrophotometer, Research Center, Faculty of pharmacy, Misr University for Science and Technology (MUST) Egypt. The values were represented in cm^{-1}. ^{1}H NMR and ^{13}C NMR spectra were recorded on Varian Gemini 300 MHz spectrophotometers using TMS as internal standard and chemical shift values were recorded in ppm on δ scale, Microanalytical Center, The Main Defence Chemical Laboratory, Egypt and Microanalytical Center, Faculty of Science, Cairo University, Egypt. Data are reported as δ

Table 3
Docking results of the target compounds in the binding site of COX-2 (4Z0L).

Compound	COX-2 (PDB ID: 4Z0L)						
	Affinity Kcal/mol	Distance (in A°) from main residue		Functional group	Interaction	2d Caption	3d Caption
14b	−16.390	2.72	Arg120	carbonyl gp.	H-acceptor	Fig. 8	Fig. 9
		3.02	Arg120	carbonyl gp.	H-acceptor		
		3.71	Val349	diazole ring	pi-H		
		4.15	Ala527	diazole ring	pi-H		
15b	−16.270	2.74	Ser119	−NH−	H-donor	Fig. 10	Fig. 11
		2.83	Arg120	carbonyl gp.	H-acceptor		
		2.82	Arg513	carbonyl gp.	H-acceptor		
		2.70	Arg513	carbonyl gp.	H-acceptor		
		4.11	Ala527	diazole ring	pi-H		
22	−13.400	2.99	Arg120	carbonyl gp.	H-acceptor	Fig. 12	Fig. 13
Indomethacin	−14.141	3.17	Arg120	carbonyl gp.	H-acceptor	Fig. 6	Fig. 7
		2.91	Arg120	carbonyl gp.	H-acceptor		
		4.37	Leu352	−COOH	H-donor		

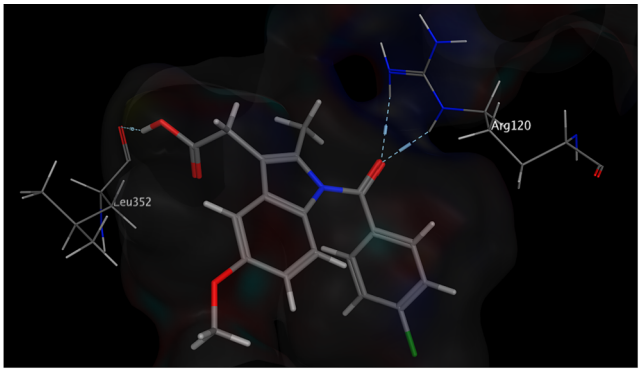

Fig. 6. Docking of Indomethacin into COX-2 (**4Z0L**).

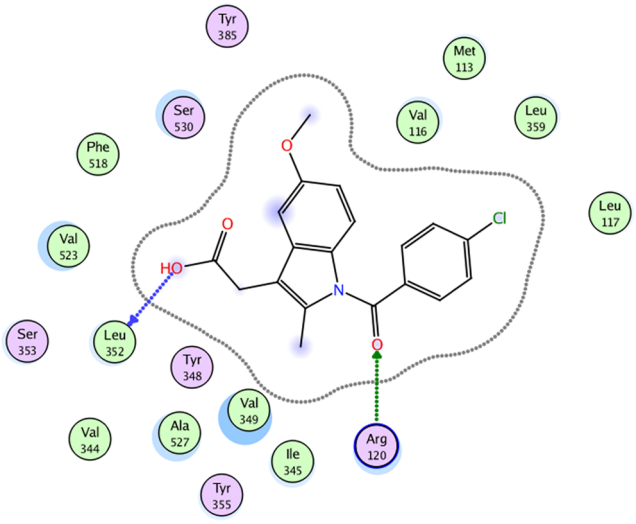

Fig. 7. Docking of Indomethacin into COX-2 (**4Z0L**).

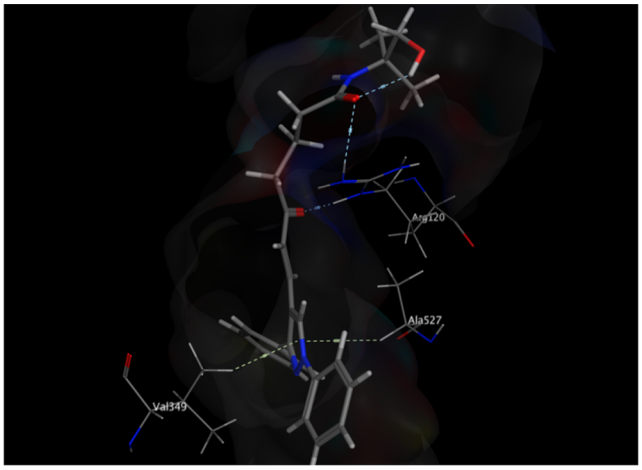

Fig. 8. Docking of **14b** into COX-2 (**4Z0L**).

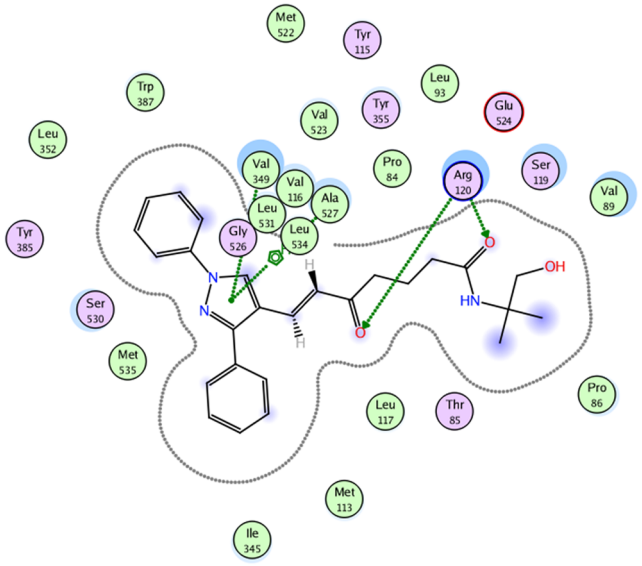

Fig. 9. Docking of **14b** into COX-2 (**4Z0L**).

values (ppm) relative to trimethylsilane (TMS) as an internal standard. The type of signal is indicated by one of the following letters: s = singlet, d = doublet, dd = doublet of doublet, t = triplet, q = quartet, m = multiplet. Mass spectra were carried out using Hewlett Packard 5988 mass spectrometer, Microanalytical Center, Cairo University, Egypt and GC Ms-QP 1000 EX mass spectrometer at Regional Center for Mycology and Biotechnology, Azhar University, Egypt. Elemental analyses were performed on Elementar Vario El III CHN analyzer (Germany) at Center for Mycology and Biotechnology, Azhar University, Egypt. Reactions were monitored by thin-layer chromatography (TLC) on TLC aluminium sheets precoated with UV fluorescent silica gel (Merck 60F 254) and were visualized using UV lamp at λ 254 nm for few seconds using benzene:acetone (9:1),

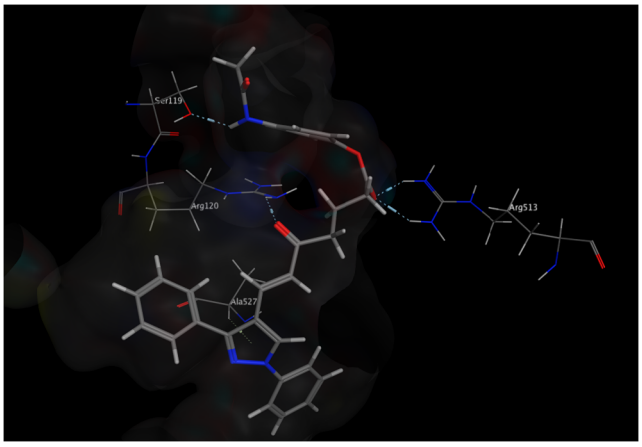

Fig. 10. Docking of **15b** into COX-2 (**4Z0L**).

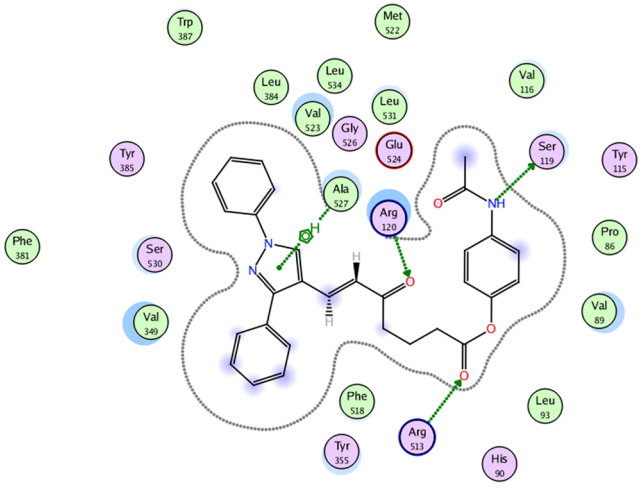

Fig. 11. Docking of **15b** into COX-2 (**4Z0L**).

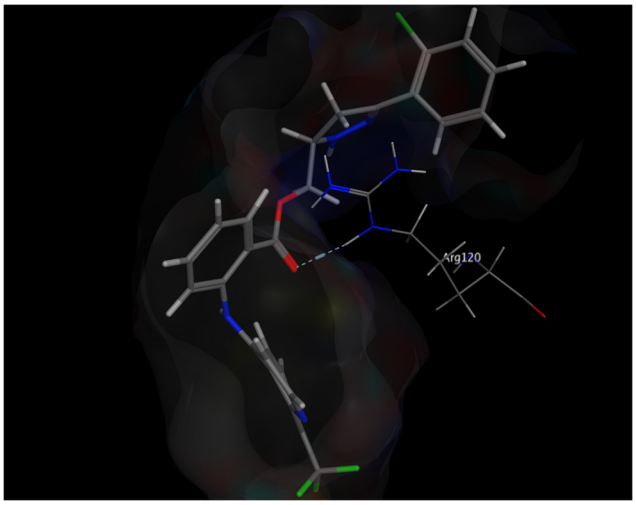

Fig. 12. Docking of **22b** into COX-2 (**4Z0L**).

chloroform: methanol (8:2) and ethyl acetate: methanol (9.8:0.2) as solvent systems.

4.1.1. General procedure of synthesis of compounds (3a-c)

A mixture of the appropriate substituted acetophenone **2a-c** (0.03 mol) and phenylhydrazine **1** (3.24 g, 2.95 mL, 0.03 mol) in absolute ethanol (30 mL) containing two drops of glacial acetic acid was heated under reflux for 15 min. The reaction mixture was allowed to cool. The formed precipitate was filtered, dried and crystallized from ethanol.

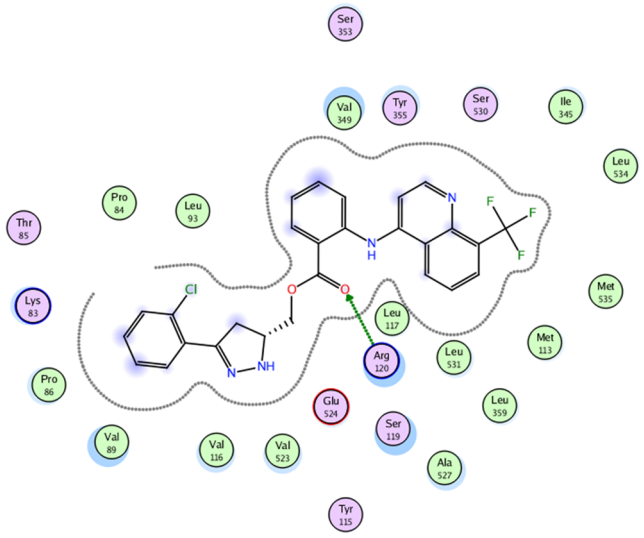

Fig. 13. Docking of **22b** into COX-2 (**4Z0L**).

*4.1.1.1. 2-Phenyl-1-(1-phenylethylidene)hydrazine (**3a**)* [60]. Yellow crystals; $C_{14}H_{14}N_2$ (210); Yield: 90%; m.p. 102–104 °C.

*4.1.1.2. 1-(1-(4-Flourophenyl)ethylidene)-2-phenylhydrazine (**6b**)* [61]. Yellow crystals; $C_{14}H_{13}FN_2$ (228); Yield: 80%; m.p. 83–85 °C.

*4.1.1.3. 1-(1-(3-Bromophenyl)ethylidene)-2-phenylhydrazine (**6c**)*[62]. Yellow crystals; $C_{14}H_{13}BrN_2$ (289); Yield: 77%; m.p. 105–107 °C.

*4.1.2. General procedure of synthesis of compounds (**7a-c**)*

A chilled solution of dimethyl formamide (2.58 g, 2.73 mL, 0.03 mol) and $POCl_3$ (5.40 g, 3.28 mL, 0.03 mol) were added dropwise on each other and stirred for 15 min at 0 °C. A solution of 2-phenyl-1-(1-substitutedphenylethylidene)hydrazines **(3a-c)** (0.01 mol) in DMF (3 mL) was added dropwise to the reaction mixture and heated at 75 °C for 5 h. The reaction mixture was cooled and a solution of 10% sodium carbonate (2 mL) was added. The obtained precipitate was filtered, washed with water (15 mL), dried and crystallized from ethanol.

*4.1.2.1. 1,3-Dipheneyl-1H-pyrazole-4-carbaldehyde (**7a**)* [60]. White crystals, $C_{16}H_{12}N_2O$ (248), Yield: 95%, m.p. 138–140 °C.

*4.1.2.2. 3-(4-Fluorophenyl)-1-phenyl-1H-pyrazole-4-carbaldehyde (**7b**)* [61]. Buff crystals, $C_{16}H_{11}FN_2O$ (266), Yield: 95%, m.p. 164–166 °C.

*4.1.2.3. 3-(3-Bromophenyl)-1-phenyl-1H-pyrazole-4-carbaldehyde (**7c**)* [62]. Buff crystals, $C_{16}H_{11}BrN_2O$ (327), Yield: 90%, m.p. 98–100 °C

*4.1.3. General procedure of synthesis of compounds (**9a-d**)*

An equimolar mixture of the appropriate1*H*-pyrazole-4-carbaldehyde (**7a-c**) (0.04 mol) and either levulinic acid or 4-acetylbutyric acid (0.04 mol each), morpholine (0.5 mL) and glacial acetic acid (1.5 mL) in dry benzene (30 mL) were heated under reflux for 8 h by using Dean Stark apparatus. The reaction mixture was allowed to cool then triturated with a mixture of acetic acid and water (1:4). The formed precipitate was filtered, dried and crystallized from ethanol.

*4.1.3.1. 6-(1,3-diphenyl-1H-pyrazol-4-yl)-4-oxohex-5-enoic acid; (**9a**).* White crystals; $C_{21}H_{18}N_2O_3$ (346); Yield: 90%; m.p. 190 °C [29].

*4.1.3.2. 6-(3-(4-fluorophenyl)-1-phenyl-1H-pyrazol-4-yl)-4-oxohex-5-enoic acid; (**9b**)*. White crystals; yield 75%; mp: 178–180 °C. IR (KBr, cm^{-1}): 3446 (OH, broad band), 3055 (C—H aromatic), 2958, 2945 (C—H aliphatic), 1710, 1656 (C=O), 1616 (C=N). ^{1}H NMR (**$CDCl_3$**) δppm: 2.74 (t, 2H, $\underline{CH_2}CH_2$—COOH), 2.97 (t, 2H, $CH_2\underline{CH_2}$—COOH), 6.66 (d, 1H, CH=$\underline{CH}$—CO), 7.20 (d, 1H, $\underline{CH}$=CH—CO), 7.50 (d, 2H, *J* = 8.4 Hz, 4-F-C_6H_4-C_2,6-H), 7.61 (s, 1H, OH, D_2O exchangeable), 7.62–7.66 (m, 5H, *N*-ArH), 7.77 (d, 2H, *J* = 8.4 Hz, 4-F-C_6H_4-C3,5-H), 8.28 (s, 1H, pyrazole–CH). EI-Mass spectrum *m/z* (relative abundance %): 366 (M + 2, 0.32%), 365 (M + 1, 0.17%), 364 (M^+, 0.35%), 77 (100%). Anal. Calcd for ($C_{21}H_{17}FN_2O_3$): C, 69.22, H, 4.70, N, 7.69. found, C, 69.28, H, 4.74, N, 7.82.

*4.1.3.3. 6-(3-(4-bromophenyl)-1-phenyl-1H-pyrazol-4-yl)-4-oxohex-5-enoic acid; (**9c**)*. Yellowish white crystals; yield 65%; mp: 158–160 °C. IR (KBr, cm^{-1}): 3452 (OH, broad band), 3061 (C—H aromatic), 2954, 2924 (C—H aliphatic), 1710, 1653 (2C=O), 1635 (C=N). ^{1}H NMR: (DMSO-d_6) δppm: 2.10 (t, 2H, $\underline{CH_2}CH_2$—COOH), 2.74 (t, 2H, $CH_2\underline{CH_2}$—COOH), 6.50 (s, 1H, CH=$\underline{CH}$—CO), 6.79 (s, 1H, $\underline{CH}$=CH—CO), 7.24–7.50 (m, 5H, *N*-ArH), 7.57–7.90 (m, 4H, 3-Br-ArH), 7.92 (s, 1H, pyrazole–CH), 8.15 (s, 1H, OH, D_2O exchangeable). EI-Mass spectrum *m/z* (relative abundance %): 427 (M + 2, 0.85%), 426 (M + 1, 1.07%), 425 (M^+, 0.59%), 55 (100%). Anal. Calcd for ($C_{21}H_{17}BrN_2O_3$): C, 59.31, H, 4.03, N, 6.59. found, C, 59.35, H, 4.04, N, 6.68.

*4.1.3.4. 7-(1,3-diphenyl-1H-pyrazol-4-yl)-5-oxohept-6-enoic acid; (**9d**)*. Yellow crystals; yield 80%; mp: 158–160 °C. IR (KBr, cm^{-1}): 3441 (OH, broad band), 3055 (C—H aromatic), 2924, 2893 (C—H aliphatic), 1712, 1651 (2C=O), 1620 (C=N). ^{1}H NMR : ($CDCl_3$) δppm: 1.99 (t, 2H, $CH_2\underline{CH_2}CH_2$—COOH), 2.46 (t, 2H, *J* = 7.2 *Hz*, $CH_2CH_2\underline{CH_2}$—COOH), 2.71 (t, 2H, *J* = 7.2 Hz, $\underline{CH_2}CH_2CH_2$—COOH, 6.57 (d, 1H, CH=$\underline{CH}$—CO), 6.63 (d, 1H, $\underline{CH}$=CH—CO), 7.33 (s, 1H, OH, D_2O exchangeable), 7.36–7.50 (m, 1H, C_6H_5-C4-H), 7.51–7.61 (m, 5H, *N*-ArH), 7.67 (d, 2H, C_6H_5-C3,5-H), 7.78 (d, 2H, C_6H_5-C_2,6-H), 8.28 (s, 1H, pyrazole–CH). EI-Mass spectrum *m/z* (relative abundance %): 362 (M + 2, 0.36%), 361 (M + 1, 1.04%), 360 (M^+, 2.01%), 77 (100%). Anal. Calcd for ($C_{22}H_{20}N_2O_3$): C, 73.32, H, 5.59, N, 7.77. found, C, 73.10, H, 6.19, N, 7.88.

*4.1.4. General procedure of synthesis of compounds (**13–15**)*

A mixture of triethylamine (1.01 g, 1.39 mL, 0.01 mol), dry methylene chloride (10 mL) and the appropriate pyrazole derivative **9aor 9d** (0.01 mol) was stirred in an ice bath at −10 °C for 15 min. Ethyl chloroformate (1.09 g, 0.78 mL, 0.01 mol) was added dropwise while stirring. To an ice cooled solution of the appropriate amine; (namely: morpholine or 2-amino-2-methyl-1-propanol) or *N*-(4-hydroxy phenyl) acetamide (0.01 mol) in dry methylene chloride (10 mL) was added dropwise over a period of 15 min and stirring was continued for 24 h at room temperature. The solvent was evaporated under vacuum till dryness and cooled. The residue was extracted twice with ethyl acetate (20 mL). The organic layer was washed with 10% hydrochloric acid (15 mL), then washed with 5% sodium hydroxide (15 mL). The organic layer was separated and dried over anhydrous sodium sulphate then filtered. The filtrate was evaporated under reduced pressure till half its volume and cooled. The crystalline solid was collected and re-crystallized from ethanol.

*4.1.4.1. 1-Morpholino-6-(1,3-diphenyl-1H-pyrazol-4-yl)hex-5-ene-1,4-dione; (**13a**)*. Orange powder; yield 90%; mp: 78–80 °C. IR (KBr, cm^{-1}): 3061 (C—H aromatic), 2960, 2856 (C—H aliphatic), 1722, 1685 (two C=O), 1635 (C=N), 1273, 1064 (C—O—C). ^{1}H NMR (**$CDCl_3$**) δppm: 2.69 (t, 2H, *J* = 6.3 Hz, $CH_2\underline{CH_2}$—CO—N—), 3.00 (t, 2H, *J* = 6.3 Hz, $\underline{CH_2}CH_2$—CO—N—), 3.46–3.57 (m, 4H, morph-$C_{2,6}$-H), 3.62–3.73 (m, 4H, morph-$C_{3,5}$-H), 6.64 (s, 1H, CH=$\underline{CH}$—CO), 6.69 (s, 1H, $\underline{CH}$=CH—CO), 7.25–7.50 (m, 5H, C_6H_5), 7.53–7.80 (m, 5H, N-C_6H_5), 8.29 (s, 1H, pyrazole–CH). Anal. Calcd for $C_{25}H_{25}N_3O_3$ (415): C, 72.27; H, 6.06; N, 10.11. Found, C, 72.29; H, 6.12; N, 10.24.

*4.1.4.2. 7-(1,3-Diphenyl-1H-pyrazol-4-yl)-1-morpholinohept-6-ene-1,5-dione; (**13b**)*. Yellow powder; yield 90%; mp: 158–160 °C. IR (KBr, cm^{-1}): 3093, 3057 (C—H aromatic), 2962, 2852 (C—H aliphatic), 1716, 1650 (two C=O), 1614 (C=N), 1269, 1064 (C—O—C). ^{13}C NMR (**$CDCl_3$**) δppm: 18.83, 19.04, 24.80, 33.55 (2C), 76.50 (2C), 76.92, 77.34, 117.52, 119.29 (2C), 125.48, 126.35, 127.21 (2C), 128.60, 128.72 (2C), 129.48 (2C), 133.36 (2C), 158.16, 187.78, 203.06. Anal. Calcd for $C_{26}H_{27}N_3O_3$ (429): C, 72.70; H, 6.34; N, 9.78. Found, C, 72.75; H, 6.36; N, 9.85.

*4.1.4.3. 6-(1,3-diphenyl-1H-pyrazol-4-yl)-N-(1-hydroxy-2-methylpropan-2-yl)-4-oxohex-5-enamide; (**14a**)*. Brownish red crystals; yield 80%; mp: 138–140 °C. IR (KBr, cm^{-1}): 3422 (OH), 3290 (NH), 3062 (C—H aromatic), 2954, 2854 (C—H aliphatic), 1739, 1663 (two C=O), 1643 (C=N). ^{1}H NMR (**$CDCl_3$**) δppm: 1.24–1.37 (m, 6H, two $\underline{CH_3}$), 2.38 (s, 1H, OH, D_2O exchangeable), 2.65 (t, 2H, *J* = 6.1 Hz, $CH_2\underline{CH_2}$—CONH—), 2.98 (t, 2H, *J* = 6.1 Hz, $\underline{CH_2}CH_2$—CO—NH—), 3.62 (s, 2H, $\underline{CH_2}$OH), 5.80 (s, 1H, NH, D_2O exchangeable), 6.60 (s, 1H, CH=$\underline{CH}$—CO), 6.64 (s, 1H, $\underline{CH}$=CH—CO), 7.36 (d, 2H, *J* = 7.0 Hz, C_6H_4-$C_{3,5}$-H), 7.45 (d, 2H, *J* = 7.8 Hz, N-C_6H_5-$C_{3,5}$-H), 7.49 (d, 2H, *J* = 7.0 Hz, C_6H_4-$C_{2,6}$-H), 7.53–7.76 (m, 2H, C_6H_4-C_4-H, N-C_6H_5-C_4-H), 7.79 (d, 2H, *J* = 7.8 Hz, N-C_6H_5-$C_{2,6}$-H), 8.28 (s, 1H, pyrazole–CH). EI-Mass spectrum *m/z* (relative abundance %): 418.00 (M + 1, 0.12), 417.00 (M^+, 0.18), 57.00 (100). Anal. Calcd for $C_{25}H_{27}N_3O_3$ (417): C, 71.92; H, 6.52; N, 10.06. Found, C, 71.89; H, 6.56; N, 10.12.

*4.1.4.4. N-(1-hydroxy-2-methylpropan-2-yl)-5-oxo-7-(1,3-diphenyl-1H-pyrazol-4-yl)hept-6-enamide; (**14b**)*. Yellowish white crystals; yield 80%; mp: 160–162 °C. IR (KBr, cm^{-1}): 3421 (OH), 3286 (NH), 3066 (C—H aromatic), 2966, 2873 (C—H aliphatic), 1730, 1662 (two C=O), 1639 (C=N). ^{1}H NMR of compound δppm: 1.29–1.37 (m, 6H, two $\underline{CH_3}$), 1.68 (s, 1H, OH, D_2O exchangeable), 1.97–2.01 (m , 2H, $CH_2\underline{CH_2}CH_2$— CO—NH—), 2.24 (t, 2H, *J* = 6.9 Hz, $CH_2CH_2\underline{CH_2}$—CO—NH—), 2.69 (t, 2H, *J* = 6.9 Hz, $\underline{CH_2}CH_2CH_2$—CO—NH—), 3.59 (s, 2H, $\underline{CH_2}$OH), 4.98 (s, 1H, NH, D_2O exchangeable), 6.58 (s, 1H, CH=$\underline{CH}$—CO), 6.63 (s, 1H, $\underline{CH}$=CH—CO), 7.34–7.39 (m, 5H, C_6H_5), 7.49 (d, 2H, *J* = 7.8 Hz, N-C_6H_5-$C_{3,5}$-H), 7.61–7.68 (m, 1H, N-C_6H_5-C_4-H), 7.79 (d, 2H, *J* = 7.8 Hz, N-C_6H_5-$C_{2,6}$-H), 8.30 (s, 1H, pyrazole–CH). Anal. Calcd for $C_{26}H_{29}N_3O_3$ (431): C, 72.37; H, 6.77; N, 9.74. Found, C, 72.40; H, 6.81; N, 9.85.

*4.1.4.5. 4-Acetamidophenyl4-oxo-6-(1,3-diphenyl-1H-pyrazol-4-yl)hex-5-enoate; (**15a**)*. Buff powder; yield 85%; mp: 158–160 °C. IR (KBr, cm^{-1}): 3317, 3209 (NH), 3059 (C—H aromatic), 2986, 2916 (C—H aliphatic), 1755, 1700, 1658 (three C=O), 1612 (C=N), 1276, 1060 (C—O—C). ^{1}H NMR δppm: 2.14 (s, 3H, NHCO$\underline{CH_3}$), 2.91 (t, 2H, *J* = 6.3 Hz, $CH_2\underline{CH_2}$COO—), 3.04 (t, 2H, *J* = 6.3 Hz, $\underline{CH_2}CH_2$COO—), 6.62 (s, 1H, CH=$\underline{CH}$—CO), 6.67 (s, 1H, $\underline{CH}$=CH—CO), 7.04 (d, 2H, *J* = 8.7 Hz, anilide-C_6H_4-$C_{3,5}$-H), 7.27–7.38 (m, 5H, C_6H_5), 7.45 (s, 1H, NH, D_2O exchangeable), 7.65–7.70 (m, 5H, N-C_6H_5), 7.79 (d, 2H, *J* = 8.7 Hz, anilide-C_6H_4-$C_{2,6}$-H), 8.29 (s, 1H, pyrazole-CH). Anal. Calcd for $C_{29}H_{25}N_3O_4$ (479): C, 72.64; H, 5.25; N, 8.76. Found, C, 72.71; H, 5.27; N, 8.84.

*4.1.4.6. 4-Acetamidophenyl-7-(1,3-diphenyl-1H-pyrazol-4-yl)-5-oxohept-6-enoate; (**15b**)*. Brownish yellow powder; yield 90%; mp: 156–158 °C. IR (KBr, cm^{-1}): 3387 (NH), 3066 (C—H aromatic), 2962 (C—H aliphatic), 1747, 1700, 1678 (three C=O), 1597 (C=N), 1270, 1060 (C—O—C).^{1}H NMR (**$CDCl_3$**) δppm: 2.06–2.13 (m, 2H, $CH_2\underline{CH_2}CH_2$COO), 2.18 (s, 3H, NHCO$\underline{CH_3}$), 2.65 (t, 2H, *J* = 7.05 Hz, $CH_2CH_2\underline{CH_2}$COO), 2.77 (t, 2H, *J* = 7.05 Hz, $\underline{CH_2}CH_2CH_2$COO), 6.59 (s, 1H, CH=$\underline{CH}$—CO), 6.65 (s, 1H, $\underline{CH}$=CH—CO), 7.23 (s, 1H, NH, D_2O exchangeable), 7.34–7.39 (m, 3H, C_6H_4-$C_{3,4,5}$-H), 7.45–7.52 (m, 5H, N-C_6H_5),

7.62–7.69 (m, 2H, C_6H_4-$C_{2,6}$-H), 7.79 (d, 2H, J = 7.8 Hz, anilide-C_6H_4-$C_{3,5}$-H), 7.87 (d, 2H, J = 7.8 Hz, anilide-C_6H_4-$C_{2,6}$-H), 8.28 (s, 1H, pyrazole–CH). Anal. Calcd for $C_{30}H_{27}N_3O_4$ (493): C, 73.01; H, 5.51; N, 8.51. Found, C, 73.05; H, 5.50; N, 8.62.

*4.1.5. General procedure for synthesis of **17a,b**.*

A solution of **7a or 7b** (0.01 mol) and 2-chloroacetophenone (1.55 g, 1.3 mL, 0.01 mol) in absolute ethanol (20 mL) was stirred with a solution of 40% potassium hydroxide (5 mL) at 0–5 °C over a period of 20 min and stirring was continued for 4 h at room temperature. The reaction mixture was poured onto ice cold water (10 mL) and neutralized with 15% hydrochloric acid (2 mL). The obtained precipitate was filtered, washed with water (15 mL), dried and crystallized from ethanol.

*4.1.5.1. 1-(2-chlorophenyl)-3-(1,3-diphenyl-1H-pyrazol-4-yl)prop-2-en-1-one, **(17a)**.* Buff powder; yield 70%; mp: 128–130 °C. IR (KBr, cm^{-1}): 3059 (C—H aromatic), 2927, 2845 (C—H aliphatic), 1668 (C═O), 1598 (C═N). ^{1}H NMR (**DMSO-d_6**) δppm: 77.12 (d, 1H, J = 6.3 Hz, CH═CH—CO), 7.17 (d, 1H, J = 6.9 Hz, CH═CH—CO), 7.20–7.26 (m, 5H, ArH), 7.27–7.33 (m, 5H, *N*-ArH), 7.36–7.41 (m, 1H, 2-Cl-C6H_4-C5-H), 7.46–7.52 (m, 1H, 2-Cl-C_6H_4-C_4-H), 7.59 (d, 1H, J = 7.8 Hz, 2-Cl-C_6H_4-C_3-H), 7.71 (d, 1H, J = 8.7 Hz, 2-Cl- C_6H_4-C_6-H), 7.87 (s, 1H, pyrazole-CH). Anal. Calcd for $C_{24}H_{17}ClN_2O$ (384.85): C, 74.90; H, 4.45; N, 7.28. Found, C, 71.88; H, 4.48; N, 7.34.

*4.1.5.2. 1-(2-Chlorophenyl)-3-(1-phenyl-3-(4-fluorophenyl)-1H-pyrazol-4-yl)prop-2-en-1-ones; **(17b)**.* Buff powder; yield 76% [19]; mp: 163–165 °C. IR (KBr, cm^{-1}): 3064, 3045 (C—H aromatic), 2926, 2866 (C—H aliphatic), 1666 (C═O), 1595 (C═N). ^{1}H NMR (**DMSO-d_6**) δppm: 7.25 (s, 2H, CH═CH—CO), 7.28–7.32 (m, 5H, N-C_6H_5), 7.41 (t, 2H, J = 7.4 Hz, 2-Cl-C_6H_4-$C_{4,5}$-H), 7.52–7.57 (m, 2H, 2-Cl-C_6H_4-$C_{3,6}$-H), 7.87–7.95 (m, 4H, 4-F-C_6H_4), 7.97 (s, 1H, pyrazole-CH). Anal. Calcd for $C_{24}H_{16}ClFN_2O$ (402.85): C, 71.55; H, 4.00; N, 6.95. Found, C, 71.62; H, 3.98; N, 7.03.

*4.1.6. General procedure for synthesis of **18a,b***

A mixture of **17a or 17b** (0.01 mol) and 99% hydrazine hydrate (1 g, 0.97 mL, 0.02 mol) was refluxed in absolute ethanol (50 mL) for 6 h. The reaction mixture was cooled, poured onto ice cold water (10 mL) and kept to stand in refrigerator overnight. The obtained precipitate was filtered, washed with water (15 mL), dried and crystallized from ethanol.

*4.1.6.1. 5-(2-chlorophenyl)-1′,3′-diphenyl-3,4-dihydro-1′H,2H-3,4′-bipyrazole; **(18a)**.* Buff powder; yield 50%; mp: 78–80 °C. IR (KBr, cm^{-1}): 3442, 3421 (NH), 3061 (C—H aromatic), 2972, 2956 (C—H aliphatic), 1637 (C═N). ^{1}H NMR (**DMSO-d_6**) δppm: 1.23–1.35 (m, 2H, pyrazolidine-CH_2), 3.85–3.93 (m, 1H, pyrazolidine-C_5-H), 6.73 (s, 1H, NH, D_2O exchangeable), 7.10–7.26 (m, 3H, 2Cl-C_6H_4-$C_{4,5}$-H, C_6H_4-C_4-H), 7.34 (d, 1H, J = 7.8 Hz, 2-Cl-C_6H_4-C_3-H), 7.36–7.42 (m, 7H, *N*-ArH, C_6H_4-$C_{3,5}$-H), 7.50 (d, 2H, J = 6.9 Hz, C_6H_4-$C_{2,6}$-H), 7.88 (d, 1H, J = 6.9 Hz, 2-Cl-C_6H_4-C_6-H), 8.53 (s, 1H, pyrazole-CH). EI-Mass spectrum *m/z* (relative abundance %): 398.10 (M^+), Anal. Calcd for $C_{24}H_{19}ClN_4$ (398.88): C, 72.27; H, 4.80; N, 14.05. Found, C, 72.29; H, 4.84; N, 14.13.

*4.1.6.2. 5-(2-chlorophenyl)-3′-(4-fluorophenyl)-1′-phenyl-3,4-dihydro-1′H,2H-3,4′-bipyrazole; **(18b)**.* Buff powder; yield 60%; mp: 83–85 °C. IR (KBr, cm^{-1}): 3439, 3427 (NH), 3064 (C—H aromatic), 2928, 2873 (C—H aliphatic), 1635 (C═N). ^{1}H NMR (**DMSO-d_6**) δppm: 1.13–1.20 (m, 2H, pyrazoline-CH_2), 3.91–3.97 (m, 1H, pyrazoline-C_5-H), 6.75 (s, 1H, NH, D_2O exchangeable), 7.01 (d, 2H, J = 6.9 Hz, 4-F-C_6H_4-$C_{2,6}$-H), 7.12–7.25 (m, 2H, 2-Cl-C_6H_4-$C_{4,5}$-H), 7.28–7.40 (m, 5H, C_6H_5), 7.44 (d, 1H, J = 6.6 Hz, 2-Cl-C_6H_4-C_3-H), 7.52 (d, 2H, J = 6.9 Hz, 4-F-C_6H_4-$C_{3,5}$-H), 7.81 (d, 1H, J = 6.0 Hz, 2-Cl-C_6H_4-C_6-H), 8.28 (s, 1H, pyrazole-CH). EI-Mass spectrum *m/z* (relative abundance %): 416.00 (M^+, 8.20), 78.45 (100). Anal. Calcd for $C_{24}H_{18}ClFN_4$ (416.88): C, 69.15; H, 4.35; N, 13.44. Found, C, 69.18; H, 4.41; N, 13.53.

*4.1.7. 2-Oxoethyl 2-[(8-(trifluoromethyl)quinolin-4-yl)amino]benzoate; **(20)***

2-Oxoethyl 2-[(8-(trifluoromethyl)quinolin-4-yl)amino]benzoate; (**20**) was synthesized according to reported procedure [40].

*4.1.8. 4-Oxo-4-(2-chlorophenyl)but-2-enyl 2-(8-(trifluoromethyl) quinolin-4-ylamino)benzoates **(21)***

A solution of **21** (3.74 g, 0.01 mol) and 2-chloro acetophenone (0.01 mol) in absolute ethanol (20 mL) was stirred with a solution of 40% potassium hydroxide (5 mL) at 0–5 °C over a period of 20 min. The reaction mixture was stirred at room temperature for 4 h then poured onto ice cold water (10 mL) and neutralized with 15% hydrochloric acid (2 mL). The obtained precipitate was filtered, washed with water (15 mL), dried and crystallized from ethanol.

Yellow powder; yield 85%; mp: 113–115 °C. IR (KBr, cm^{-1}): 3404 (NH), 3099, 3078 (C—H aromatic), 2972, 2926 (C—H aliphatic), 1734, 1678 (two C═O), 1616 (C═N), 1259, 1070 (C—O—C). ^{1}H NMR (**$CDCl_3$**) δppm: 4.49 (s, 2H, —OCH_2), 6.92 (s, 1H, CH═CH), 7.16 (s, 1H, CH═CH), 7.35–7.46 (m, 2H, C_6H_4-$C_{3,5}$-H), 7.54–7.59 (m, 2H, C_6H_4-$C_{2,4}$-H), 7.62–7.68 (m, 3H, quinoline-C_3-H& 2-Cl-C_6H_4- $C_{4,5}$-H), 7.86 (d, 1H, J = 6.0 Hz, 2-Cl-C_6H_4-C_6-H), 8.10 (d, 1H, J = 6.0 Hz, 2-Cl-C_6H_4-C_3-H), 8.31–8.37 (m, 2H, quinoline-$C_{5,6}$-H), 8.57–8.70 (m, 2H, quinoline-$C_{2,7}$-H), 9.91(s, 1H, NH, D_2O exchangeable). EI-Mass spectrum *m/z* (relative abundance %): 512.00 (M + 2, 1.86), 78.00 (100). Anal. Calcd for $C_{27}H_{18}ClF_3N_2O_3$ (510.89): C, 63.48; H, 3.55; N, 5.48. Found, C, 63.52; H, 3.60; N, 5.61.

*4.1.9. Methyl (4,5-dihydro-3-(2-chloro phenyl)-1H-pyrazole-5-yl)-2-(8-(trifluoromethyl)quinolin-4-ylamino)benzoate **(22)***

A solution of **21** (0.01 mol) and 99% hydrazine hydrate (1 g, 0.97 mL, 0.02 mol) was refluxed in absolute ethanol (50 mL) for 6 h. The reaction mixture was cooled, poured onto ice cold water (10 mL) and kept to stand in refrigerator overnight. The obtained precipitate was filtered, washed with water (15 mL), dried and crystallized from ethanol.

Yellow crystals; yield 85%; mp: 200–202 °C. IR (KBr, cm^{-1}): 3450, 3332 (NH), 3076 (C—H aromatic), 2983 (C—H aliphatic), 1650 (C═O), 1616 (C═N), 1267, 1072 (C—O—C). ^{1}H NMR (**$CDCl_3$**) δppm: 1.23–1.28 (m, 2H, pyrazoline-CH_2), 3.72–3.75 (m, 3H, pyrazoline-C_5-H& OCH_2), 6.92 (s, 1H, pyrazoline-NH, D_2O exchangeable), 7.04–7.21 (m, 3H, C_6H_4-$C_{3,5}$-H & quinoline-C_3-H), 7.53–7.59 (m, 3H, 2-Cl-C_6H_4-$C_{4,5,6}$-H), 7.62–7.67 (m, 2H, C_6H_4-$C_{2,4}$-H), 8.10–8.19 (m, 2H, quinoline-$C_{5,6}$-H), 8.36 (d, 1H, J = 8.1 Hz, 2-Cl-C_6H_4-C_3-H), 8.87–8.89 (m, 2H, quinoline-$C_{2,7}$-H), 9.85 (s, 1H, quinoline-NH, D_2O exchangeable). Anal. Calcd for $C_{27}H_{20}ClF_3N_4O_2$ (524.92): C, 61.78; H, 3.84; N, 10.67. Found, C, 61.79; H, 3.89; N, 10.75.

4.2. Pharmacology

Pharmacological screening of ten synthesized compounds **(13a, 13b, 14a, 14b, 15a, 15b, 17, 18a, 21, 22)** was carried out in the animal facility of Faculty of Pharmacy, Cairo University, Pharmacology Department, Egypt. Anti-inflammatory activities of all novel synthesized compounds were assessed according to the method described by Winter *et al.* [63], while analgesic activities were carried out by writhing test according to the method described by Hegazi *et al.* [69].

4.2.1. Acute Anti-inflammatory procedure (Carrageenan-induced paw edema)

The screening for anti-inflammatory activity was carried out by rat paw oedema test according to the method described by Winter *et al.* [63]. Fifty five albino rats of both sexes weighing 120–150 g which

were obtained in the animal facility of Faculty of Pharmacy, Cairo University. The equipment used was "Dial micrometer model 9120-1206 Baey, Sussex, England". Rats were divided into eleven groups, each group consisted of 5 rats per cage. The rats were kept fastened for 24 h prior to the experiment, but they were allowed free access to water [65] under constant temperature; 30 °C and 12 h light/dark cycle. Control group received the excepients (1 mL tween 80) followed by carrageenan after 1 h. Reference standard group received Indomethacin (10 mg/kg) orally (using intragastric tube) and the other groups received the tested compounds (10 mg/kg) orally followed by carrageenan after 1 h. Acute inflammation was induced one hour after drug administration by injection of 1% (0.05 mL) of carrageenan sodium subcutaneously into the sub planter region of the right hind paw. The thickness of the injected paw was measured (from dorsal to ventral surfaces) immediately after carrageenan injection and after (1, 2 and 4 h) by using a micrometer [66]. The size of oedema was expressed as the increase in the thickness in mm after carrageenan injection. The percentage inhibition of oedema thickness at each time interval was calculated according to the equation as **[(Tc − Tt)/Tc] × 100**, where **Tc** and **Tt** are the mean increase in thickness of the carrageenan injected paw of the control group and drug treated one; respectively [64]. Then the potencies of compounds were calculated after four hours of carrageenan injection, where the % oedema inhibition reached its maximum.

4.2.2. Analgesic effect evaluation procedure (Writhing test)

The screening for analgesic activity was carried out by writhing test according to the method described by Kamel *et al.* [64]. Fifty five mice of both sexes weighing 25–30 g were obtained in the animal facility of Faculty of Pharmacy, Cairo University. They were divided into eleven groups, each group consisted of 5 mices per cage. Animals were kept fastened for 24 h prior to the experiment, but they were allowed free access to water [67] under constant temperature 30 °C and 12 h light/dark cycle. Control group received the excepients (1 mL Tween 80) followed by 0.6% acetic acid solution (10 mL/kg) I.P. after one hour. Reference standard group received Indomethacin (10 mg/kg) orally (using intragastric tube) and the other groups received the tested compounds (10 mg/kg) orally followed by injection of 0.6% acetic acid solution (10 mL/kg) I.P. after one hour [24]. Stretching movements were counted for 15 min immediately after the acetic acid injection. The percentage of inhibition of writhes number was calculated as follows: **% Inhibition of writhes number = [(Nc − Nt)/Nc] × 100** where **Nc** and **Nt** are mean of number of writhes in the control group and drug group; respectively. Then the potencies of compounds (P is a ratio of % writhing movements inhibition of test compound to reference drug) were calculated.

4.3. Docking study

Docking studies were made using COX-2 co-crystallized with the native ligand (PDB ID: **4Z0L**). Poses for compounds **14b, 15b, 22** and **Indomethacin** were scored by initial rescoring methodology (London dG) and the final rescoring methodology (London dG) after docking by placement using Triangle Matcher protocol and post-placement refinement was Rigid Receptor. The best scoring pose of the docked compounds was recognized. Receptor-ligand interactions of the complexes were examined in 2D and 3D styles, **(**Table 1**)**. X-ray crystal structure of COX-2 complexed with with a nido-dicarbaborate-containing indomethacin derivative at 2.29 Å resolution. All molecular modeling calculations and docking studies were carried out using 'Molecular Operating Environment 2019.0101' software (MOE of Chemical Computing Group Inc., on a Core i5 2.2 GHz workstation) running on a Windows 10 PC. The X-ray crystallographic structure of cyclooxygenase 2 (PDB ID: 4Z0L) was downloaded from the protein data bank (http://www.rcsb.org/) [68]. The enzyme was prepared for docking study by removal of chain B,C and D of its dimmers, water molecules, and ligands that are not involved in the binding. The enzyme was then prepared using quick preparation protocol in MOE with default options.

To ensure the validity of the docking protocol, re-docking of the co-crystallized the native ligand into the active site was performed. The coordinates of the best scoring docking pose of the native ligand was compared with its coordinates in the co-crystallized PDB file based on the binding mode and root mean square deviation (rmsd). Which showed a near perfect alignment with the original ligand as obtained from the X-ray resolved PDB file. The re-docked ligand showed rmsd of 0.3971 between the docked pose and the co-crystallized ligand (energy score (S) = −14.641 kcal/mol).

The docked compounds (Three compounds: **14b, 15b** and **22**) and the positive control **Indomethacin** were prepared for docking by applying the following steps:

- 2D structures of the docked ligands were built using Marvin Sketch and copied to MOE.
- 3D protonation of the structure.
- Running conformational analysis using systemic search.
- Selecting the least energetic conformer.
- Applying the same docking protocol used with ligand.

Declaration of Competing Interest

The authors have declared no conflict of interest.

References

[1] L. Chen, H. Deng, H. Cui, J. Fang, Z. Zuo, J. Deng, Y. Li, X. Wang, L. Zhao, Inflammatory responses and inflammation-associated diseases in organs, Oncotarget 9 (6) (2018) 7204.

[2] H. Ohshima, M. Tatemichi, T. Sawa, Chemical basis of inflammation-induced carcinogenesis, Arch. Biochem. Biophys. 417 (1) (2003) 3–11.

[3] L. Brubaker, L. Kendall, E. Reina, Multimodal analgesia: a systematic review of local NSAIDs for non-ophthalmologic postoperative pain management, Int. J. Surgery 32 (2016) 158–166.

[4] G. Dannhardt, W. Kiefer, Cyclooxygenase inhibitors–current status and future prospects, Eur. J. Med. Chem. 36 (2) (2001) 109–126.

[5] M. Ezawa, D.S. Garvey, D.R. Janero, S.P. Khanapure, L.G. Letts, A. Martino, R.R. Ranatunge, D.J. Schwalb, D.V. Young, Design of a heteroaryl modified, 1, 5-disubstituted pyrazole cyclooxygenase-2 (COX-2) selective inhibitor, Lett. Drug Des. Disc. 2 (1) (2005) 40–43.

[6] W. Badri, K. Miladi, Q.A. Nazari, H. Greige-Gerges, H. Fessi, A. Elaissari, Encapsulation of NSAIDs for inflammation management: overview, progress, challenges and prospects, Int. J. Pharm. 515 (1–2) (2016) 757–773.

[7] H. Jick, Risk of upper gastrointestinal bleeding and perforation associated with individual non-steroidal anti-inflammatory drugs, The Lancet. 343 (8900) (1994) 769–772.

[8] S. Trelle, S. Reichenbach, S. Wandel, P. Hildebrand, B. Tschannen, P.M. Villiger, M. Egger, P. Jüni, Cardiovascular safety of non-steroidal anti-inflammatory drugs: network meta-analysis, BMJ 342 (2011) c7086.

[9] K.M. Hatt, A. Vijapura, I.B. Maitin, E. Cruz, Safety considerations in prescription of NSAIDs for musculoskeletal pain: a narrative review, PM&R 12 (2018) 1404–1411.

[10] P. Pirlamarla, R.M. Bond, FDA labeling of NSAIDs: review of nonsteroidal anti-inflammatory drugs in cardiovascular disease, Trends Cardiovasc. Med. 26 (8) (2016) 675–680.

[11] P.M. Kearney, C. Baigent, J. Godwin, H. Halls, J.R. Emberson, C. Patrono, Do selective cyclo-oxygenase-2 inhibitors and traditional non-steroidal anti-inflammatory drugs increase the risk of atherothrombosis? Meta-analysis of randomised trials, Bmj 332 (7553) (2006) 1302–1308.

[12] H.E. Vonkeman, M.A. van de Laar, Nonsteroidal anti-inflammatory drugs: adverse effects and their prevention, Seminars in arthritis and rheumatism, vol. 39, no. 4, WB Saunders, 2010, pp. 294–312.

[13] S. Wongrakpanich, A. Wongrakpanich, K. Melhado, J. Rangaswami, A comprehensive review of non-steroidal anti-inflammatory drug use in the elderly, Aging Disease 9 (1) (2018) 143.

[14] L. Cuzzolin, M. Dal Cerè, V. Fanos, NSAID-induced nephrotoxicity from the fetus to the child, Drug Saf. 24 (1) (2001) 9–18.

[15] C.A. Naughton, Drug-induced nephrotoxicity, Am. Fam. Physician 78 (2008) 6.

[16] J.D. Greenberg, M.C. Fisher, J. Kremer, H. Chang, E.D. Rosenstein, M. Kishimoto, S. Lee, Y. Yazici, A. Kavanaugh, S.B. Abramson, The COX-2 inhibitor market withdrawals and prescribing patterns by rheumatologists in patients with gastrointestinal and cardiovascular risk, Clin. Exp. Rheumatol. 27 (2009) 395.

[17] K. Nakata, T. Hanai, Y. Take, T. Osada, T. Tsuchiya, D. Shima, Y. Fujimoto, Disease-modifying effects of COX-2 selective inhibitors and non-selective NSAIDs in osteoarthritis: a systematic review, Osteoarthr. Cartilage 26 (10) (2018) 1263–1273, https://doi.org/10.1016/j.joca.2018.05.021.

[18] M.E. Shoman, M. Abdel-Aziz, O.M. Aly, H.H. Farag, M.A. Morsy, Eur. J. Med. Chem.

44 (2009) 3068.
[19] M.M. Alam, A. Marella, M. Akhtar, A. Husain, M.S. Yar, O.P. Tanwar, R. Saha, S. Khanna, S. Shafi, Acta Pol. Pharm. 70 (2013) 435.
[20] B. Cottineau, P. Toto, C. Marcot, A. Pipaud, J. Chenault, Bioorg. Med. Chem. 12 (2002) 2105.
[21] A.E. Rashad, M.I. Hegab, R.E. Abdel-Megeid, N. Fathalla, F.M. Abdel-Megeid, Eur. J. Med. Chem. 44 (2009) 3285.
[22] S.M. Riyadh, T.A. Farghaly, M.A. Abdallah, M.M. Abdalla, M.R. Abd El-Aziz, Eur. J. Med. Chem. 45 (2010) 1042.
[23] S.A. Rostom, M.A. Shalaby, M.A. El-Demellawy, Eur. J. Med. Chem. 38 (2003) 959.
[24] M. Bonesi, M.R. Loizzo, G.A. Statti, S. Michel, F. Tillequin, F. Menichini, The synthesis and Angiotensin Converting Enzyme (ACE) inhibitory activity of chalcones and their pyrazole derivatives, Bioor. & Med. Chem. Lett. 20 (6) (2010) 1990–1993.
[25] N. Gökhan-Kelekçi, S. Yabanoğlu, E. Küpeli, U. Salgın, Ö. Özgen, G. Uçar, E. Yeşilada, E. Kendi, A. Yeşilada, A.A. Bilgin, A new therapeutic approach in Alzheimer disease: some novel pyrazole derivatives as dual MAO-B inhibitors and antiinflammatory analgesics, Bioor. & Med. Chem. 15 (17) (2007) 5775–5786.
[26] H.M. Faidallah, K.A. Khan, A.M. Asiri, Synthesis and biological evaluation of new 3, 5-di (trifluoromethyl)-1, 2, 4-triazolesulfonylurea and thiourea derivatives as antidiabetic and antimicrobial agents, J. Fluorine Chem. 132 (11) (2011) 870–877.
[27] Ş.G. Küçükgüzel, S. Şenkardeş, Recent advances in bioactive pyrazoles, Eur. J. Med. Chem. 97 (2015) 786–815.
[28] J.V. Faria, P.F. Vegi, A.G. Miguita, M.S. dos Santos, N. Boechat, A.M. Bernardino, Recently reported biological activities of pyrazole compounds, Bioorg. Med. Chem. 25 (21) (2017) 5891–5903.
[29] M.F. Khan, M.M. Alam, G. Verma, W. Akhtar, M. Akhter, M. Shaquiquzzaman, The therapeutic voyage of pyrazole and its analogs: a review, Eur. J. Med. Chem. 120 (2016) 170–201.
[30] K. Karrouchi, S. Radi, Y. Ramli, J. Taoufik, Y. Mabkhot, F. Al-aizari, Synthesis and pharmacological activities of pyrazole derivatives: a review, Molecules 23 (1) (2018) 134.
[31] C.H. Tseng, C.W. Tung, S.I. Peng, Y.L. Chen, C.C. Tzeng, C.M. Cheng, Discovery of pyrazolo [4, 3-c] quinolines derivatives as potential anti-inflammatory agents through inhibiting of NO production, Molecules 23 (5) (2018) 1036.
[32] M.A. Chowdhury, K. Abdellatif, Y. Dong, D. Das, M.R. Suresh, E. Knaus, Bioorg. Med. Chem. Lett. 18 (2008) 6138.
[33] G. Friedrich, T. Rose, K. Rissler, Determination of lonazolac and its hydroxy and O-sulfated metabolites by on-line sample preparation liquid chromatography with fluorescence detection, J. Chromatogr. B 766 (2) (2002) 295–305.
[34] M.A. Ismail, J. Lehmann, D.A.A. El Ella, A. Albohy, K.A. Abouzid, Med. Chem. Res. 18 (2009) 725–744.
[35] A. Kalgutkar, A. Marnett, B. Crews, R. Remmel, L. Marnett, J. Med. Chem. 43 (2000) 2860.
[36] A. Qandil, Prodrugs of nonsteroidal anti-inflammatory drugs (NSAIDs), more than meets the eye: a critical review, Int. J. Mol. Sci. 12 (2012) 17244–17274.
[37] C.K. Ong, R.A. Seymour, P. Lirk, A.F. Merry, Combining paracetamol (acetaminophen) with nonsteroidal antiinflammatory drugs: a qualitative systematic review of analgesic efficacy for acute postoperative pain, Anesth. Analg. 110 (2010) 1170.
[38] V. Muralidharan, C. Asha Deepti, S. Raja, A review on anti-inflammatory potential of substituted pyrazoline derivatives synthesised from chalcones, Int. J. Pharm. Pharm. Sci. 10 (2018) 9.
[39] N. Desai, V. Joshi, K.R. Ajpara, H.V. Aghani, H. Satodiya, J. Fluorine Chem. 142 (2012) 67.
[40] G.H. Hegazy, A. Taher, A. El-Zaher, Arch. Pharm. 338 (2005) 378.
[41] L. Knorr, Einwirkung von acetessigester auf phenylhydrazin, Eur. J. Inorg. Chem. 16 (1883) 2597–2599.
[42] X. Deng, N.S. Mani, Reaction of N-monosubstituted hydrazones with nitroolefins: a novel regioselective pyrazole synthesis, Org. Lett. 8 (16) (2006) 3505–3508.
[43] L. Porter, F. Cervantes-Lee, H. Murray III, Monatshefte fÃ¼r Chemie/Chem. Mon. 124 (1993) 775–782.
[44] P. Rathelot, N. Azas, H. El-Kashef, F. Delmas, C. Di Giorgio, P. Timon-David, J. Maldonado, P. Vanelle, Eur. J. Med. Chem. 37 (2002) 671–679.
[45] A. Kumar, O. Prakash, M. Kinger, S.P. Singh, Can. J. Chem. 84 (2006) 438–442.
[46] P.K. Sharma, N. Chandak, P. Kumar, C. Sharma, K.R. Aneja, Eur. J. Med. Chem. 46 (2011) 1425–1432.
[47] L.-L. Xu, C.-J. Zheng, L.-P. Sun, J. Miao, H.-R. Piao, Eur. J. Med. Chem. 48 (2012) 174–178.
[48] L. De Luca, G. Giacomelli, S. Masala, A. Porcheddu, Synlett 2004 (2004) 2299–2302.
[49] K. Abouzid, P. Frohberg, J. Lehmann, M. Decker, J. Med. Chem. 3 (2007) 433.
[50] J. Mahajan, H. Araujo, J. Org. Chem. 36 (1971) 1832-1832.
[51] N.A. Osman, A.H. Mahmoud, M. AllarÃ, R. Niess, K.A. Abouzid, V.D. Marzo, A.H. Abadi, Bioorg. Med. Chem. 18 (2010) 8463–8477.
[52] B.P. Bandgar, S.S. Gawande, R.G. Bodade, N.M. Gawande, C.N. Khobragade, Bioorg. Med. Chem. 17 (2009) 8168–8173.
[53] B. Insuasty, A. Tigreros, F.n. Orozco, J. Quiroga, R. AbonÃa, M. Nogueras, A. Sanchez, J. Cobo, Bioorg. Med. Chem. 18 (2010) 4965–4974.
[54] C. Khunt, V.M. Khedkar, R.S. Chawda, N.A. Chauhan, A.R. Parikh, E.C. Coutinho, Bioorg. Med. Chem. Lett. 22 (2012) 666–678.
[55] F.A. Ragab, N.M. Abdel Gawad, H.H. Georgey, M.F. Said, Eur. J. Med. Chem. 63 (2013) 645–654.
[56] A. Rayar, M.S. Veitía, C. Ferroud, An efficient and selective microwave-assisted Claisen-Schmidt reaction for the synthesis of functionalized benzalacetones, SpringerPlus 4 (1) (2015) 221.
[57] V. Muralidharan, C. Asha, Deepti, S. Raja, Int. J. Pharm. Pharm. Sci. 10 (2018) 9.
[58] B. Insuasty, A. Montoya, D. Becerra, J. Quiroga, R. Abonia, S. Robledo, Y. Upegui, Eur. J. Med. Chem. 67 (2013) 252.
[59] W. Neumann, S. Xu, M.B. Sárosi, M.S. Scholz, B.C. Crews, K. Ghebreselasie, E. Hey-Hawkins, Chem. Med. Chem. 11 (2) (2016) 175–178.
[60] P. Rathelot, N. Azas, H. El-Kashef, F. Delmas, C. Giorgio, P. Timon, J. Maldonado, P. Vanelle, Eur. J. Med. Chem. 37 (2002) 671.
[61] S. Jadhav, S. Shirame, V. Sonawane, M. Hublikar, K. Onawane, R. Shaikh, Int. J. Pharm. Bio. Sci. 4 (2013) 390.
[62] G. Friedrich, T. Rose, K. Rissler, J. Chromatogr. B 766 (2002) 295–305.
[63] C.A. Winter, E.A. Risley, G.W. Nus, Exper. Bio. Med. 111 (1962) 544.
[64] K. Gyires, Z. Torma, The use of the writhing test in mice for screening different types of analgesics, Archives internationales de pharmacodynamie et de therapie 267 (1) (1984) 131–140.
[65] A.A. Bekhit, H.M. Ashour, Y.S. Abdel-Ghany, A. Bekhit, A. Baraka, Eur. J. Med. Chem. 43 (43) (2008) 456.
[66] S. Venkataraman, S. Jain, K. Shah, N. Upmanyu, Acta Pol. Pharm. 67 (2010) 361.
[67] M. Amir, S. Kumar, Ind. J. Chem., Sect. B 44 (2005) 2532.
[68] M.B. Sárosi, J. Mol. Model. 24 (7) (2018) 150.
[69] G. Hegazy, G. Kamel, Synthesis of new Ester Entities of NSAIDs with Nitric Oxide Releasing Properties, Life Sci. J. 9 (3) (2012) 1113–1120.